

# Coculture of Stem Cells from Apical Papilla and Human Umbilical Vein Endothelial Cell Under Hypoxia Increases the Formation of Three-Dimensional Vessel-Like Structures *in Vitro*

Changyong Yuan, BDS,<sup>1-3,\*</sup> Penglai Wang, MDS,<sup>3,\*</sup> Lifang Zhu, MDS,<sup>1,2</sup>  
Waruna Lakmal Dissanayaka, BDS, PhD,<sup>1,2</sup> David William Green, PhD,<sup>4</sup>  
Edith H.Y. Tong, PhD,<sup>4</sup> Lijian Jin, DDS, PhD,<sup>5</sup> and Chengfei Zhang, DDS, PhD<sup>1,2</sup>

The success of bioengineered dental pulp depends on two principles, (1) whether the transplanted tissue can develop its own vascular endothelial tubule network and (2) whether the host vasculature can be induced to penetrate the bioengineered pulp replacement and conjoin. Major inductive molecules that participate in laying down blood vessels include vascular endothelial growth factor (VEGF), ephrinB2, and hypoxia-inducible factor 1 $\alpha$  (HIF-1 $\alpha$ ). Being able to modulate the genes encoding these angiogenic molecules is a therapeutic target in pulp regeneration for endogenous blood vessel formation, prevention of graft rejection, and exclusion of infection. Once implanted inside the root canal, bioengineered pulp is subjected to severe hypoxia that causes tissue degeneration. However, short-term hypoxia is known to stimulate angiogenesis. Thus, it may be feasible to prime dental cells for angiogenic activity before implantation. Stem cells from apical papilla (SCAP) are arguably one of the most potent and versatile dental stem cell populations for bioengineering pulp *in vitro*. Our study aimed to investigate whether coculture of SCAP and human umbilical vein endothelial cells (HUVECs) under hypoxia promotes the formation of endothelial tubules and a blood vessel network. In addition, we clarified the interplay between the genes that orchestrate these important angiogenic molecules in SCAP under hypoxic conditions. We found that SCAP cocultured with HUVEC at a 1:5 ratio increased the number of endothelial tubules, tubule lengths, and branching points. Fluorescence staining showed that HUVEC formed the trunk of tubular structures, whereas SCAP located adjacent to the endothelial cell line, resembling the pericyte location. When we used CoCl<sub>2</sub> (0.5 mM) to induce hypoxic environment, the expression of proteins, HIF-1 $\alpha$  and VEGF, and transcript of ephrinB2 in SCAP was upregulated. However, minimal VEGF levels in supernatants of HUVEC and coculture Petri dishes were detected, suggesting that VEGF secreted by SCAP might be used by HUVEC to accelerate the formation of vessel-like structures. Taken together, we revealed that artificial hypoxia stimulates angiogenic responses in SCAP for possible use in engineering dental pulp replacements. Our results may help to delineate the optimal therapeutic target to promote angiogenesis so that future bioengineered pulp replacements integrate faster and permanently within the host.

## Introduction

**T**EETH WITH INFECTED or necrotic pulp because of trauma, caries, and operative procedures are mainly treated by removal of the entire pulp and subsequent replacement with artificial fillings.<sup>1</sup> Loss of vitalized dental pulp invariably makes the tooth more susceptible to repeated

infection, fracture, and eventually ejection from its socket. Engineered living tissue replacements are alternative because they ensure restoration of whole tooth health by preventing infection and maintaining structural integrity. Numerous regenerative strategies are currently under investigation. The most common strategy implements stem cell-laden frameworks to accelerate the production of new

<sup>1</sup>Comprehensive Dental Care, Endodontics, Faculty of Dentistry, The University of Hong Kong, Hong Kong, China.

<sup>2</sup>HKU Shenzhen Institute of Research and Innovation, Hong Kong, China.

<sup>3</sup>Dental Implant Center, Xuzhou Stomatological Hospital, Xuzhou, China.

<sup>4</sup>Oral Biosciences and <sup>5</sup>Periodontology, Faculty of Dentistry, The University of Hong Kong, Hong Kong, China.

\*These two authors contributed equally to this work.

pulp merged with dentine.<sup>2-4</sup> Five distinctive and well-characterized stem cell populations have been discovered with strong clinical potential to generate various new permanent dental tissues *in vitro*. These populations include stem cells from apical papilla (SCAP), periodontal ligament stem cells, dental pulp stem cells (DPSCs), stem cells from human exfoliated deciduous teeth, and dental follicle stem cells (DFSCs).<sup>5,6</sup> SCAP and DFSCs are less studied than DPSCs, but they are the most potent and perhaps the most plastic type of stem cells.<sup>7</sup> As therapeutic stem cells, SCAP appear to be the most reliable because they are easily harvested from extracted premolars or wisdom teeth and have the ability to differentiate into osteogenic, odontogenic, adipogenic, angiogenic, and neurogenic lineages.<sup>8,9</sup>

Pulp connective tissue occupies the entire root canal into the center of each tooth, which is surrounded by a case of dentine. There is only one blood supply line to the entire pulp, which originates from the tight opening of the apical foramen.<sup>10</sup> This blood supply provides 80% of the total blood supply to the pulp tissue. In severe traumatic injuries or inflammation at any region of the tooth, the neurovascular bundle can be severely disrupted, leading to ischemia in the pulp tissue itself.<sup>11</sup> The small space leading into the pulp cavity is also a major obstacle for dental pulp regeneration, because any engineered pulp tissues needs heavy neovascularization and rapid infusion into the host vascular system immediately after transplantation.<sup>10</sup> Without normal oxygen levels, dental pulp cell metabolism, nourishment, and behavior are all compromised.<sup>12</sup>

Therefore, all transplanted pulp tissue replacements must be given a blood supply to ensure healthy and optimal function. A strategy to assist with blood supply is to induce angiogenesis at the host tissue interface. One method to reinitiate angiogenesis is stimulating the expression of the hypoxia-inducible factor (HIF) family of transcription regulators.<sup>13</sup> Thus, although hypoxia should be avoided within any bioengineered construct, a degree of oxygen limitation is actually necessary to prime exogenous dental cells for vasculogenic and angiogenic responses.

Ubiquitously expressed HIF-1 consists of two basic heterodimeric proteins,  $\alpha$  subunit (HIF-1 $\alpha$ ) and  $\beta$  subunit (HIF-1 $\beta$ ). HIF-1 $\alpha$  expression is rapidly activated under hypoxic conditions (<5% oxygen), whereas HIF-1 $\beta$  is constitutively expressed in an oxygen-independent manner.<sup>14</sup> Accumulation and translocation of HIF-1 $\alpha$  into the nucleus is a major driving force for angiogenesis.<sup>12-15</sup> EphrinB2 and its receptor, EphB4, have emerged as critical regulators in the development of the vascular system and contribute to the function of adult vasculature with comparable importance to vascular endothelial growth factor (VEGF) and angiopoietins.<sup>15,16</sup> EphrinB2 is expressed in adult arteries, arterioles and capillaries, whereas EphB4 is expressed predominantly in endothelial cells (ECs) of venous origin. Under physiological and pathological conditions, ephrinB2 expression and phosphorylation are increased in angiogenic vessels. This pattern of EphB4/ephrinB2 expression is closely related to EC growth, survival, migration, and angiogenesis.<sup>16</sup> Recent studies have revealed that various Eph/ephrin family members are expressed during tooth development.<sup>17</sup> When cocultured with human umbilical vein endothelial cell (HUVEC), DPSCs significantly enhance and stabilize tube-like structures generated by the assembled HUVEC populations.<sup>18</sup> After treatment with soluble fms-like ty-

rosine kinase-1 (sFlt-1, also referred to as sVEGFR-1) to block VEGF binding to VEGFR-2, DPSCs exhibit decreased expression of ephrinB2 and subsequently induce less vessel formation *in vivo*.<sup>19</sup> However, the precise role has not been revealed for ephrinB2 from dental stem cells in angiogenesis.

In this study, we aimed to investigate (1) whether coculture of SCAP and HUVEC under hypoxia promotes the formation of endothelial tubules and a blood vessel network, (2) the expression profiles of angiogenesis-related genes encoding HIF-1 $\alpha$ , VEGF, and EphB4/ephrinB2 molecules in SCAP under hypoxia, (3) the individual and synergistic roles of SCAP angiogenic activities when cocultured with HUVEC.

## Materials and Methods

### *Isolation, culture, and characterization of SCAP*

After obtaining informed consent, SCAP were isolated from freshly extracted human third molars with immature roots (aged 18–25 years) as described previously.<sup>8</sup> Briefly, the root apical papilla was removed from the end and digested in a solution of 3 mg/mL collagenase type I (Gibco-Invitrogen, Carlsbad, CA) and 4 mg/mL dispase (Gibco-Invitrogen) for 1 h at 37°C. Then, the cells were passed through a 70- $\mu$ m strainer (BD Biosciences, Franklin Lakes, NJ) to obtain a single cell suspension. The cells were seeded in 75-cm<sup>2</sup> culture flasks containing  $\alpha$ -minimum essential medium ( $\alpha$ -MEM; Gibco BRL, Gaithersburg, MD) supplemented with 15% fetal bovine serum (Gibco BRL), 0.292 mg/mL glutamine (Sigma, St. Louis, MO), 100 U/mL penicillin (Sigma), 100  $\mu$ g/mL streptomycin (Sigma), and cultured at 37°C with 5% CO<sub>2</sub>. HUVEC were obtained commercially (ScienCell Research Laboratories, San Diego, CA) and cultured in EC medium (ScienCell Research Laboratories) at 37°C with 5% CO<sub>2</sub>. Before using SCAP for experiments, the freshly isolated cells were assessed for their stemness by flow cytometric analysis of the expression of CD73, CD90, CD105, STRO-1, and CD45. In addition, the multilineage differentiation capacity of SCAP was confirmed using osteogenic and odontogenic, adipogenic, and neurogenic induction media. Passage 3–6 cells were used in experiments to ensure retention of their stem cell qualities.

### *Hypoxic culture conditions*

SCAP grown to 80–90% confluence were trypsinized and counted. For hypoxic conditions, cells were seeded at a density of  $3 \times 10^5$  cells/mL in six-well plates and cultured for 3 days to achieve 80–90% confluence. Then, the cells were starved with serum-free medium for 12 h followed by incubation with 0.5 mM CoCl<sub>2</sub> (Sigma). At various time points, mRNA and proteins were harvested from the cells for subsequent analyses. All experiments were performed in triplicate.

For experiments with HIF-1 $\alpha$  inhibitors, the cells were pretreated with 80  $\mu$ M YC-1 (AG Scientific, San Diego, CA) for 2 h before hypoxic stimulation. Normoxic and hypoxic cultures without inhibitors were used as controls.

### *In vitro matrigel angiogenesis assay*

To investigate whether coculture of SCAP and HUVEC under hypoxia promotes formation of endothelial tubules and a blood vessel network, tubular formation assay was

carried out as described previously.<sup>18</sup> Briefly, HUVECs ( $6 \times 10^5$ ) alone or cocultured with SCAP (SCAP:HUVEC, 1:5) were seeded in six-well plates precoated with Matrigel (1.5 mL/well; BD Biosciences).  $\text{CoCl}_2$  (0.5 mM) was added to the medium of experimental group to mimic hypoxic environment. Images were obtained under an inverted phase-contrast microscope after 6 h and analyzed with the Leica Qwin Image Processing and Analysis Software (Version V2.6; Leica, Cambridge, United Kingdom). Tubule length, junctional areas, and the number of branching points were measured in images at  $10 \times$  magnification ( $n = 5$ ). Cell lysates and supernatants were collected and detected using western blot and enzyme-linked immunosorbent assay (ELISA). To distinguish HUVEC and SCAP in vessel-like structures, CellTracker™ fluorescent probes (Invitrogen, Carlsbad, CA) were used to label them. SCAPs were stained with orange fluorescence and HUVECs were stained with green fluorescence. Images were obtained under fluorescence microscope.

*Cell sorting after coculture of HUVEC and SCAP*

To detect VEGF mRNA expression in HUVEC and SCAP after coculture, Dynabeads® CD31 Endothelial Cell (Life Technologies AS, Oslo, Norway) was used to separate HUVEC from SCAP. Briefly, cells were harvested using Dispase (Corning, Tewksbury, MA) after 3 h of coculture in Matrigel. Then, 1 mL single cell suspension was mixed with 25  $\mu\text{L}$  prewashed magnetic beads, and incubated for 20 min at 4°C under gentle rotation. The tube was then placed in a magnet for 2 min. Finally, the supernatant containing the cocultured SCAP (co-SCAP) was transferred to a new tube, and bead-bound HUVEC (co-HUVEC) was left on the tube wall. 350  $\mu\text{L}$  Buffer RLT Plus RNeasy Plus lysis buffer (QIAGEN GmbH, Hilden, Germany) was used to lyse cell pellet. Real-time PCR was performed to detect VEGF gene expression in SCAP and HUVEC, respectively. SCAP or HUVEC incubated alone in Matrigel was used as control.

*Real-time polymerase chain reaction*

Total RNA was extracted using an RNeasy Mini Kit (Qiagen, Hilden, Germany). RNA concentrations were quantified using a NanoDrop ND-1000 spectrophotometer (NanoDrop Technologies, Wilmington, DE). Total RNA (2  $\mu\text{g}$ ) was then used to synthesize cDNA by the SuperScript® VILO™ Master Mix (Invitrogen). Quantitative real-time polymerase chain reaction (PCR) was performed using an ABI Prism 7000 Sequence Detection System (Applied Biosystems, Carlsbad, CA) with SYBR Green (Applied Biosystems). All samples in 96-well plates were run in triplicate. Each well contained 2  $\mu\text{L}$  cDNA diluted at 1:3 for a total reaction volume of 20  $\mu\text{L}$ . PCR conditions were initial denaturation for 10 min at 95°C, followed by 40 cycles of denaturation for 15 s at 95°C, and annealing for 1 min at 60°C or 64°C (primer specific). Amplicons were subjected to melting point analyses by heating for 1 min from 95°C to 60°C. All primers were purchased from Sigma and are listed in Table 1. The mRNA levels of HIF-1 $\alpha$ , VEGF, EphB4, and ephrinB2 were determined and normalized to the GAPDH internal control. Standards and samples were run in triplicate.

TABLE 1. PRIMER SEQUENCES USED FOR REAL-TIME POLYMERASE CHAIN REACTION

<i>Gene</i>	<i>Primers</i>
HIF-1 $\alpha$	For: GGCGC GAACGACAAGAAAAAG Rev: CCTTATCAAGATGCGAACTCACA
VEGF	For: CAAAAACGAAAGCGCAAGAAA Rev: GCGGGCACCAACGTACAC
EphB4	For: CCTTCCTGCGGCTAAACGAC Rev: GTTGACTAGGATGTTGCGAG
EphrinB2	For: CCTCTCCTCAACTGTGCCAAA Rev: CCCAGAGGTTAGGGCTGAATT
GAPDH	For: GGCATGGACTGTGGTCATGAG Rev: TGCACCACCAACTGCTTAGC

HIF-1 $\alpha$ , hypoxia-inducible factor 1 $\alpha$ ; VEGF, vascular endothelial growth factor.

*Western blot analyses*

To assess the effects of hypoxia on the synthesis of HIF-1 $\alpha$ , EphB4, and ephrinB2 proteins, SCAP grown in 10-cm culture dishes were treated with 0.5 mM  $\text{CoCl}_2$  for 0, 2, 4, 8, and 24 h. For inhibition experiments, the cells were pretreated with 80  $\mu\text{M}$  YC-1 for 2 h followed by hypoxic stimulation.

After each treatment, the cells were rinsed twice with phosphate buffered saline. Then, total protein was obtained using M-PER protein extraction buffer containing 3 $\times$  protease inhibitor cocktail (Thermo Scientific, Rockford, IL). Cellular proteins were quantified by a BCA kit (Pierce, Rockford, IL), and then separated on 7.5% or 12% polyacrylamide gels followed by transfer onto the Immun-Blot polyvinylidene fluoride membranes (GE Healthcare Life Sciences, Little Chalfont, United Kingdom). The membranes were blocked for 1 h with 5% nonfat milk powder in Tris-phosphate buffer containing 0.05% Tween 20 (TBST). Then, the membranes were incubated overnight at 4°C with primary antibodies, including anti-HIF-1 $\alpha$  polyclonal antibody (1:400; BD Transduction Laboratories, San Jose, CA), anti-EphB4 polyclonal antibody (1:100; Abcam, Hong Kong, China), anti-ephrinB2 polyclonal antibody (1:200; Abcam), and anti- $\beta$ -actin monoclonal antibody (1:800; Santa Cruz Biotechnology, Santa Cruz, CA). After five washes with TBST for 5 min each, the membranes were incubated with horseradish peroxidase-conjugated secondary antibodies (Cell Signaling Technology, Danvers, MA) for 2 h at room temperature, and then washed three times in TBST for 5 min each. The target protein signal was detected using ECL (Thermo Scientific).

*Enzyme-linked immunosorbent assay*

VEGF expression was measured by Quantikine ELISA (R&D Systems, Minneapolis, MN). Briefly, the supernatants were collected and centrifuged to remove particulates. We pipetted 500  $\mu\text{L}$  of Calibrator Diluent RD5K into each tube, and used stock solution to produce a dilution series, then added 50  $\mu\text{L}$  of Assay Diluent RD1W and 200  $\mu\text{L}$  of standard, control, or sample to each well. After washing three times, 200  $\mu\text{L}$  of VEGF Conjugate was added to each well and incubated at room temperature for 2 h, then 200  $\mu\text{L}$  of

the substrate solution was added to each well, protected from light, and incubated it at room temperature for 20 min. Finally, we added 50  $\mu$ L of Stop Solution to each well, and determined the optical density of each well using a microplate reader at 450 and 570 nm.

#### Statistical analysis

Relative expression levels of genes, tubular junctional areas, and tubule lengths were presented as the mean  $\pm$  standard deviation. Data were analyzed using the Student's *t*-test or one-way analysis of variance with a *post hoc* Tukey test to compare between groups as appropriate.  $p < 0.05$  was considered statistically significant.

## Results

### Isolated SCAP exhibit stem cell properties

SCAP were a typical fibroblastic spindle shape when cultured in  $\alpha$ -MEM. Flow cytometric analyses showed that SCAP highly expressed CD73, CD90, and CD105, and weakly expressed CD45, whereas 26.35% of SCAP expressed STRO-1 (Fig. 1A). Neurogenic induction caused morphological changes in the cells and expression of the neurogenic marker  $\beta$ III-tubulin (Fig. 1B). Oil Red O staining revealed that lipid droplets had formed in experimental groups after 3 weeks of adipogenic induction (Fig. 1C). Alizarin Red staining showed obvious mineralization of SCAP after 4 weeks of odontogenic and osteogenic induction (Fig. 1D).

### Coculture of SCAP and HUVEC under hypoxia enhances the formation of vessel-like structures

HUVECs seeded on Matrigel alone formed a small number of vessel-like structures after 6 h (Fig. 2A), whereas those cocultured with SCAP (Fig. 2B) or incubated under hypoxic conditions (Fig. 2C) formed more vessel-like structures. When HUVECs and SCAPs were cocultured under hypoxia, we detected the most extensive lattice of vessel-like structures among all groups (Fig. 2D). Using immunofluorescence microscopy, we found that HUVEC formed the trunk of tubular structures (Fig. 2E), and SCAP located adjacent to the EC line (Fig. 2F). Compared with the HUVEC control group, the other three groups had longer tubule lengths (Fig. 2G) and higher number of branching points (Fig. 2H). The tubular junctional areas of hypoxia and coculture groups were also smaller than those of the HUVEC alone groups (Fig. 2I).

### VEGF expression in SCAP and HUVEC

The average concentration of VEGF protein in supernatants secreted by SCAP under normoxia was 205 pg/mL (Fig. 3A). When SCAPs were incubated in hypoxia, VEGF expression increased and its concentration reached to 1249 pg/mL (Fig. 3A). VEGF mRNA expression in SCAP under hypoxia was upregulated time dependently. The highest VEGF mRNA level was observed after 4 h of incubation under hypoxia (5.8-fold, Fig. 4B). Compared with SCAP, HUVEC secreted less VEGF protein (15 pg/mL). Surprisingly, when SCAP was cocultured with HUVEC, VEGF concentration in supernatants was also very low

(35 pg/mL). To reveal its mechanism, we used magnetic beads to separate HUVEC from SCAP after 3 h of coculture; real-time PCR results showed that mRNA expression between SCAP and co-SCAP had no significant difference, but was upregulated in co-SCAP under hypoxia (Fig. 3B). VEGF mRNA levels in HUVEC, co-HUVEC, or co-HUVEC under hypoxia were much lower than in SCAP, co-SCAP, or co-SCAP under hypoxia (Fig. 3B).

### HIF-1 $\alpha$ and ephrinB2 in SCAP under hypoxia are upregulated

Real-time PCR results showed that HIF-1 $\alpha$  mRNA was upregulated after 4 h of hypoxia (Fig. 4A). The HIF-1 $\alpha$  protein was barely detectable under normoxia, but its expression was induced obviously under hypoxic conditions and reached a maximum after 4 h of exposure (15.7-fold compared with the 2 h group, Fig. 5).

EphrinB2 mRNA expression was induced quickly, peaked after 2 h (2.25-fold), and then fluctuated until 8 h of hypoxia (Fig. 4C). Subsequently, ephrinB2 mRNA expression decreased to a normal level after 12 h. Western blot results showed that there were no significant changes of ephrinB2 protein levels in normoxia and hypoxia groups (Fig. 5A). EphB4, which is a cognate receptor of ephrinB2, also showed steady protein levels after hypoxic induction (Fig. 5A), whereas EphB4mRNA expression decreased constantly after hypoxic induction (Fig. 4D).

### Hypoxia-dependent upregulation of VEGF and ephrinB2 expression is mediated by HIF-1 $\alpha$

To directly demonstrate that the upregulation of ephrinB2 and VEGF expression under hypoxia was mediated by HIF-1 $\alpha$ , we used YC-1 to suppress HIF-1 $\alpha$  expression. After a series of preliminary experiments, we found that 80  $\mu$ M YC-1 suppressed HIF-1 $\alpha$  expression thoroughly (Fig. 6A). After treatment with 80  $\mu$ M YC-1, the hypoxia-dependent upregulation of HIF-1 $\alpha$ , VEGF, and ephrinB2 expression was abrogated (Fig. 6B, C).

## Discussion

Rapid and sufficient blood perfusion is necessary for the integration and survival of *in vitro* bioengineered tissue constructs.<sup>20</sup> Several strategies have been developed to accelerate angiogenesis and thus overcome the strict diffusion limits imposed inside bioengineered tissues that are thicker than 500  $\mu$ m. Such strategies include the provision of various proangiogenic factors,<sup>21,22</sup> genetic modification of cells to overproduce growth factors,<sup>23,24</sup> specific biomaterial design to mimic the extracellular matrix with high porosities,<sup>25</sup> and embedding ECs into engineered tissue constructs.<sup>26,27</sup> However, the time required for EC migration, angiogenic sprouting, and vasculogenesis is still too long to guarantee the viability of bioengineered tissue after implantation and for it to merge and fuse with host tissue.<sup>28</sup> It has been reported that extensive networks are formed at day 5 when engineered replacements are prevascularized with HUVEC before implantation.<sup>29</sup> The space of the root canal is encapsulated by dentin in the center of each tooth with only a single blood supply from its apical end.<sup>30</sup> This anatomical limitation poses even more challenges for rapid integration

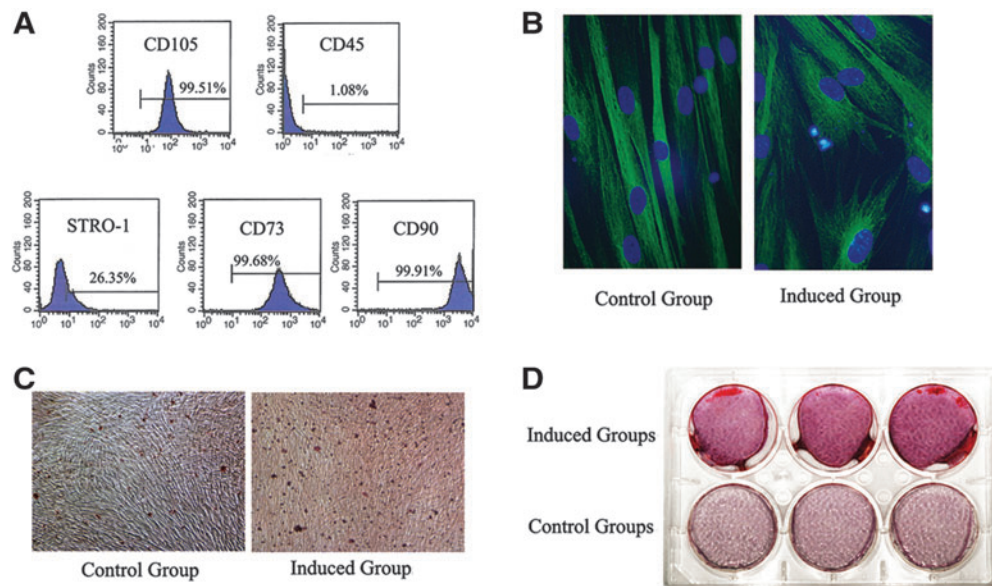


**FIG. 1.** Characterization of stem cells from apical papilla (SCAP). (A) Flow cytometry results of mesenchymal stem cell markers CD105, CD45, STRO-1, CD73, and CD90. (B) Immunofluorescence imaging of  $\beta$ III-tubulin after 3 weeks of induction ( $\times 100$ ). (C) Oil Red O staining of lipid droplets after 3 weeks of induction ( $\times 4$ ). (D) Alizarin Red detection of mineralization after 4 weeks of induction.

into the host vascular system after transplantation. Therefore, it is essential to develop novel approaches to significantly reduce the time needed for rapid anastomosis and enhance functional angiogenesis between *in vitro* bioengineered tissue and host tissues.

Similar to the results of our previous study,<sup>18</sup> we found that coculture of SCAP and HUVEC at a ratio of 1:5 increases tubule formation. However, the mechanism is still unclear. Previous studies have shown that ECs and DPSCs secrete an array of growth factors that are beneficial for the

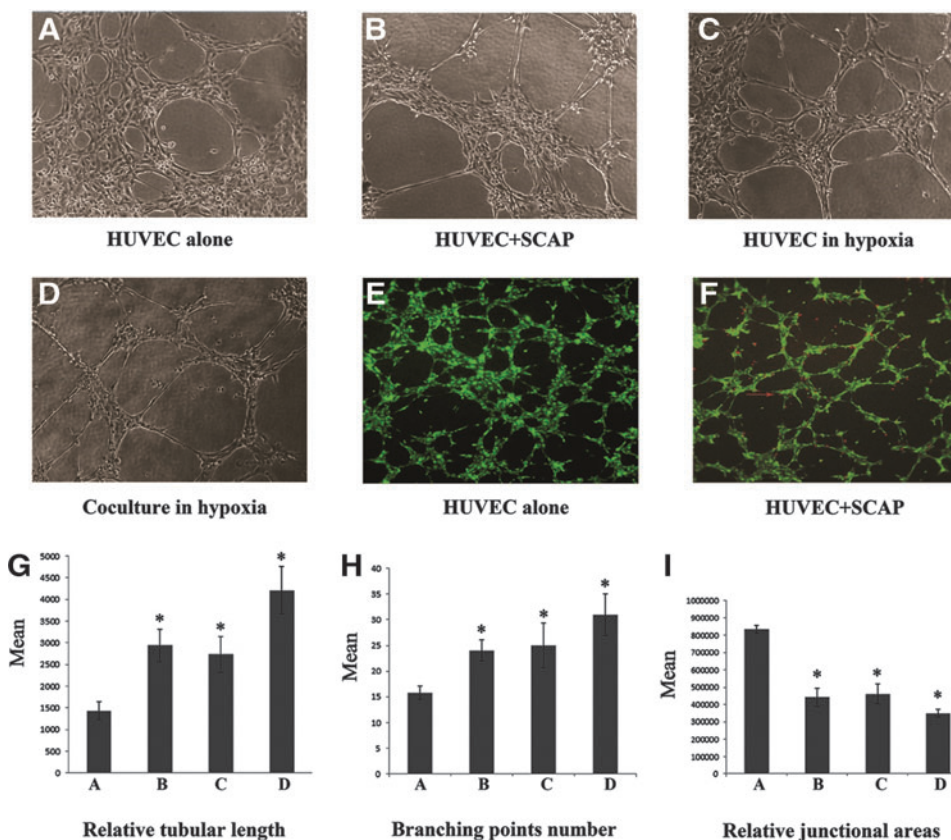


**FIG. 2.** *In vitro* Matrigel angiogenesis assay. (A–F) Phase-contrast images ( $\times 10$ ) of cells at 6 h after seeding on Matrigel. Arrow showed SCAPs (Red) which located in confluent areas. (G–I) Graphic representations of the (G) relative tubular length, (H) number of branching points, and (I) relative junctional area. Data are presented as the mean  $\pm$  standard deviation ( $n = 5$ ). \* $p < 0.05$  versus human umbilical vein endothelial cells (HUVECs) alone group.

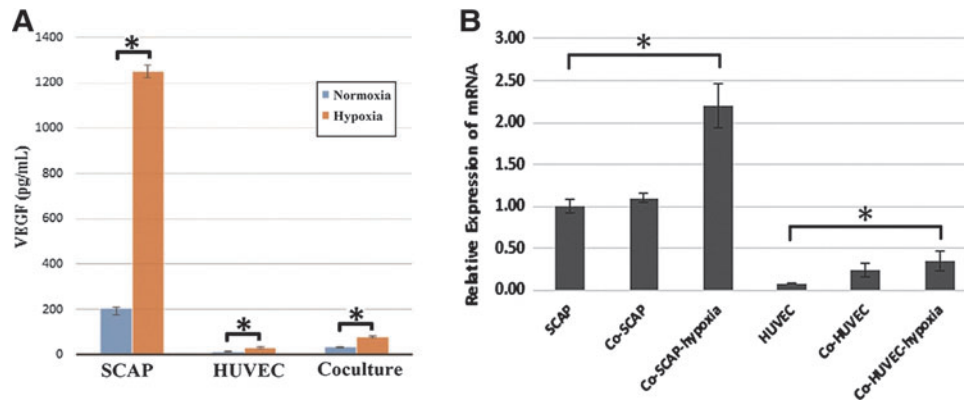
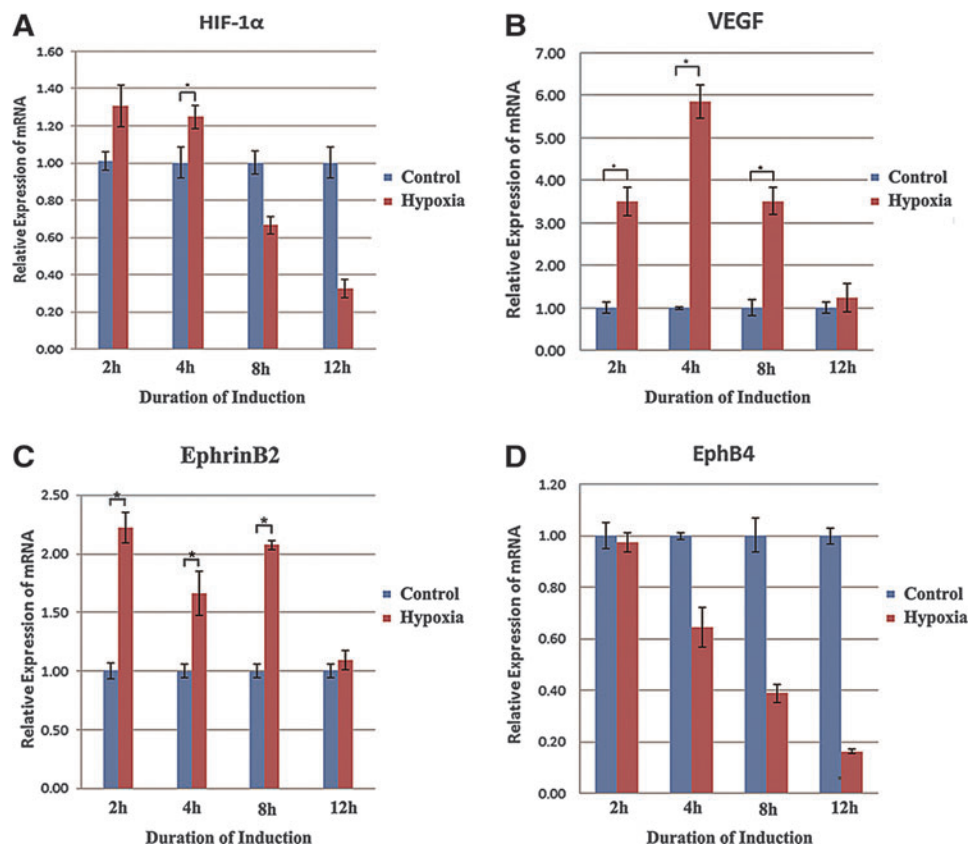


**FIG. 3.** Protein and mRNA expression of vascular endothelial growth factor (VEGF) in SCAP and HUVEC. **(A)** Enzyme-linked immunosorbent assay (ELISA) was performed to detect VEGF protein concentration in supernatant of SCAP, HUVEC, and coculture of them under normoxia and hypoxia. **(B)** Magnetic beads were used to separate HUVEC from SCAP after 3 h of coculture under normoxia and hypoxia. VEGF mRNA expression in each cell type was detected using Real-time polymerase chain reaction (PCR) assay. SCAP isolated culture was regarded as control group, which were standardized to 1 ( $*p < 0.05$ ).

growth, differentiation, and functions of other cell types.<sup>31–35</sup> ECs secrete insulin growth factor-1, endothelin-1, fibroblast growth factor, platelet-derived growth factor, transforming growth factor- $\beta$  and bone morphogenic protein-2,<sup>32</sup> which are established inducers of DPSC proliferation and differentiation.<sup>33,34</sup> In addition, DPSCs secrete VEGF that enhances the survival and differentiation of ECs.<sup>35</sup> Furthermore, in a coculture tubular formation assay, DPSCs carry out the functions of pericyte-like cells and are located adjacent to ECs to

stabilize tube-like structures.<sup>19</sup> To demonstrate the colocalization of SCAP and HUVEC in tubular formation assay, we stained the cells in orange and green fluorescence, respectively. The results showed that HUVEC formed the trunk of tubular structures, whereas SCAP located adjacent to the ECs, resembling the pericyte location. SCAP are very similar to DPSCs, both express mesenchymal markers, such as CD13, CD29, CD44, CD73, CD90, CD105, CD146, and STRO-1, and have multilineage differentiation abilities.<sup>5</sup> These findings

**FIG. 4.** Relative expression levels of **(A)** hypoxia-inducible factor 1 $\alpha$  (HIF-1 $\alpha$ ), **(B)** VEGF, **(C)** ephrinB2, and **(D)** EphB4 at various time points under normoxia and hypoxia as detected by real-time polymerase chain reaction (PCR). Values were normalized to GAPDH expression ( $*p < 0.05$ ).



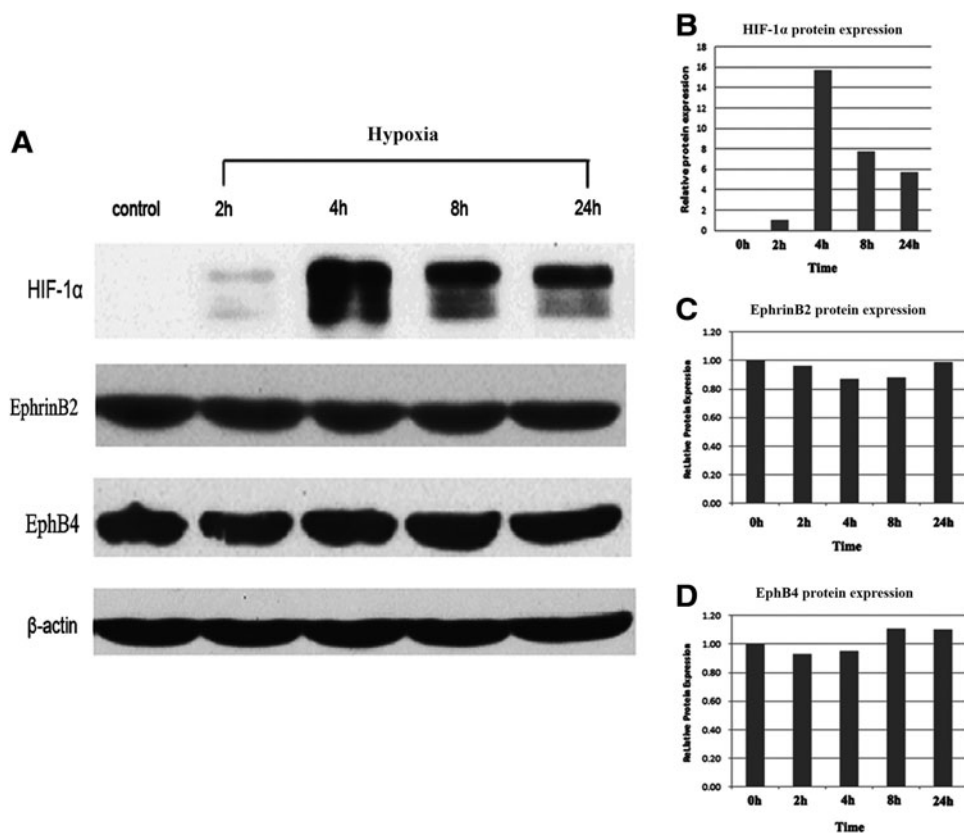


**FIG. 5.** Protein expression of HIF-1α, VEGF, ephrinB2 and EphB4. (A) Protein expression of HIF-1α, ephrinB2, and EphB4 at various time points under normoxia and hypoxia as detected by western blot analyses. (B–D) Relative protein expression of HIF-1α, VEGF and ephrinB2 versus control group at the indicated time point.

may explain why more vascular tubules reminiscent of blood vessel networks were formed in cocultures of SCAP and HUVEC at a ratio of 1:5.

In our study, we also found that coculture of HUVEC and SCAP under hypoxia formed more vessel-like structures.

Since hypoxia always occur in implanted prevascularized pulp tissue constructs, we used CoCl<sub>2</sub> to mimic hypoxic environment and explore its underlying mechanism. As expected, we found that the expression of HIF-1α and VEGF in SCAP increased significantly under hypoxia.

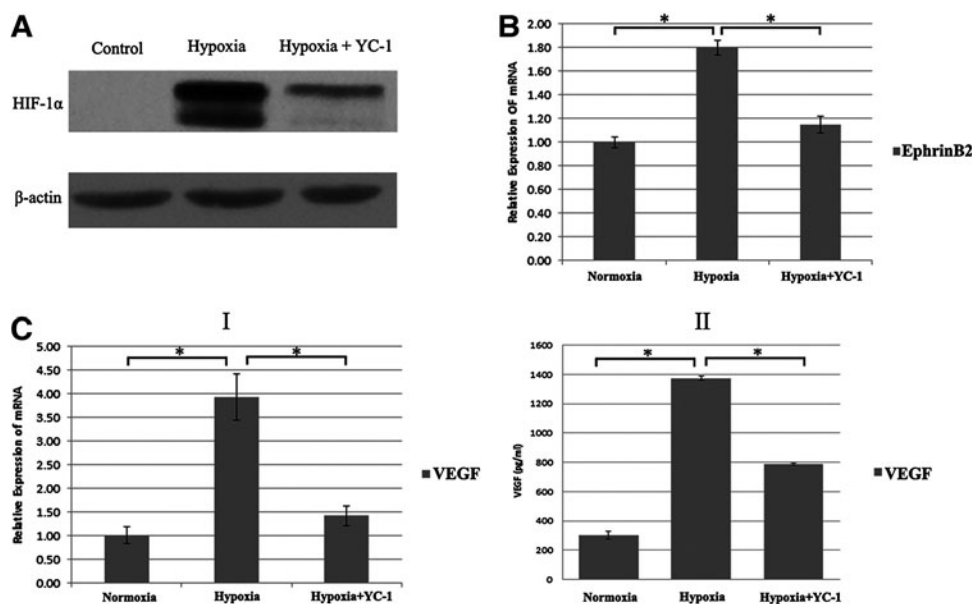


**FIG. 6.** Expression of HIF-1α, VEGF, and ephrinB2 after inhibition of HIF-1α expression by YC-1. (A) Western blotting showed that overexpression of HIF-1α protein was blocked by 80 μM YC-1 after 4h under hypoxia. (B) Real-time PCR results showed that the upregulated mRNA expression of ephrinB2 in SCAPs was reduced by 80 μM YC-1 after 2h under hypoxia. (C) VEGF mRNA and protein expression after inhibition of HIF-1α expression (I) Real-time PCR results showed that the increased mRNA expression of VEGF in SCAPs was inhibited by 80 μM YC-1 after 2h under hypoxia. (II) ELISA showed that the VEGF protein concentration was also reduced by 80 μM YC-1 after 24h under hypoxia.

VEGF is a particularly strong stimulator of angiogenesis and its expression increased dramatically at the mRNA level (5.8-fold) and protein level (6.1-fold). Compared to SCAP, HUVEC secreted less VEGF protein. Interestingly, when we cocultured SCAP and HUVEC, VEGF concentration of supernatant was found to be very low as well. We speculated that VEGF secreted by SCAP may be metabolized by HUVEC to accelerate the formation of vessel-like structures. To support our hypothesis, magnetic beads were used to separate HUVEC from SCAP after 3 h of coculture, and real-time PCR was performed to detect VEGF gene expression. Results showed that VEGF mRNA level in co-SCAP and co-HUVEC were upregulated when they were cocultured in hypoxia. It confirmed that the secretion of VEGF by SCAP under coculture condition was not inhibited. Acceleration of vessel-like structure formation in the coculture groups indicated that the secretion of VEGF be metabolized by HUVEC. However, further study is needed to elaborate the molecular processes.

Previous studies have demonstrated that vascular ephrinB2 and its cognate EphB receptors perform critical functions in vascular development, and increased expression of ephrinB2 in a number of tumor categories may be involved in tumor angiogenesis.<sup>36–38</sup> However, the expression of ephrinB2 under hypoxia is still controversial. Vihanto *et al.*<sup>15</sup> suggested that hypoxia upregulates the expression of EphB4 and ephrinB2 in hypoxemic mouse skin. Conversely, Reissenweber *et al.*<sup>39</sup> showed that hypoxic conditions do not influence the expression or synthesis of EphA2, EphB4, ephrinA1, ephrinA5, and ephrinB2 in four different human melanoma cell lines *in vitro*.

In contrast, we found that the mRNA expression of ephrinB2 in SCAP was upregulated significantly under hypoxia, but its protein expression remained low and steady. Furthermore, the mRNA expression of EphB4 in SCAP decreased constantly after hypoxic induction, but its protein expression remained steady. There are presumably several reasons for this contradictory phenomenon. First, the *in vitro* models lack the regulatory effects of a real hypoxic microenvironment expected *in vivo*, including secreted molecules and interacting cells.<sup>39</sup> Second, there are many complicated and varied posttranscriptional modifications involved in translating mRNA into protein, which are not yet sufficiently defined to accurately calculate protein concentrations from mRNA.<sup>40</sup> Changes in the expression of proteins in response to altered oxygen levels may be caused primarily by differences in the translational efficiency of the mRNAs rather than changes in the mRNA levels.

We also demonstrated that the upregulated expression of VEGF and ephrinB2 was related to HIF-1 $\alpha$ , which is the major regulator of gene transcription in response to oxygen deprivation.<sup>41</sup> After HIF-1 $\alpha$  was blocked by YC-1, the mRNA and protein expression of VEGF in SCAP under hypoxia decreased accordingly, and the mRNA expression of ephrinB2 was also downregulated. These results indicate that the overexpression of VEGF and ephrinB2 induced by hypoxia is dependent on HIF-1 $\alpha$ . This finding is in perfect agreement with the study of Vihanto *et al.*,<sup>15</sup> but contradicts the conclusion of Sohl *et al.*<sup>42</sup> The latter suggested that neither HIF-1 $\alpha$  nor HIF-2 $\alpha$  are responsible for hypoxic induction of ephrinB2 expression in mouse arterial ECs. There is a strong possibility that (1) the different cells used or (2)

the distinct *in vivo* and *in vitro* environments account for these contradictory results.

The correlation of EphB4/ephrinB2 and VEGF expression in different cell lines is still obscure. Das *et al.*<sup>43</sup> indicated that stimulation of human hepatic stellate cells with either ephrinB2 Fc or EphB4 Fc significantly increases VEGF mRNA levels, whereas small interfering RNAs for ephrinB2 and EphB4 inhibit this increase. They further observed that ephrinB2 stimulates phosphorylation of extracellular signal-regulated kinases, which are key cell survival and proliferation proteins, to regulate VEGF-A expression through HIF-1 phosphorylation.<sup>44</sup> Another study showed that VEGF upregulates Delta-like 4 (DLL4) and presenilin expression, and increases activation of Notch4, leading to upregulation of ephrinB2 and downregulation of EphB4 in venous ECs.<sup>45</sup> In contrast, Yang *et al.*<sup>46</sup> found that VEGF-A inhibits expression of EphB4 and stimulates expression of DLL4, but does not stimulate either Notch or ephrinB2 expression in adult venous ECs. Pretreatment with a VEGFR-2 neutralizing antibody abolishes VEGF-stimulated downregulation of EphB4, but not the upregulation of DLL4. These results indicate that multiple molecules are possibly implicated in the crosstalk of SCAP and HUVEC, which are currently under investigation by our research team.

In summary, we found that coculture of HUVEC and SCAP under hypoxia increases the formation of vessel-like structures. To reveal the precise molecular mechanism responsible for this observation, we found that hypoxia upregulates both mRNA and protein expression of HIF-1 $\alpha$  and VEGF as well as mRNA expression of ephrinB2 in SCAP. Furthermore, overexpression of VEGF and ephrinB2 in SCAP under hypoxia is dependent on HIF-1 $\alpha$ . These findings indicate that VEGF might play a critical role in tissue angiogenesis under hypoxia as it does normally, but the lack of corresponding secretion of ephrinB2 protein will influence permanent angiogenesis of implanted tissues under hypoxia.<sup>43</sup> Therefore, we should focus on strategies that increase the protein expression of ephrinB2 in SCAP under hypoxia, and further explore the correlation between VEGF and ephrinB2 expression.

#### Acknowledgments

This work was supported by a grant from the National Nature Science Foundation of China (81271135) to C.Z.

#### Disclosure Statement

No competing financial interests exist.

#### References

1. Ricucci, D. Apical limit of root canal instrumentation and obturation, part 1. Literature review. *Int Endod J* **31**, 384, 1998.
2. Zhu, X., Zhang, C., Huang, G.T., Cheung, G.S., Disanayaka, W.L., and Zhu, W. Transplantation of dental pulp stem cells and platelet-rich plasma for pulp regeneration. *J Endod* **38**, 1604, 2012.
3. Ishizaka, R., Iohara, K., Murakami, M., Fukuta, O., and Nakashima, M. Regeneration of dental pulp following pulpectomy by fractionated stem/progenitor cells from bone marrow and adipose tissue. *Biomaterials* **33**, 2109, 2012.



4. Huang, G.T., Yamaza, T., Shea, L.D., Djouad, F., Kuhn, N.Z., Tuan, R.S., and Shi, S. Stem/progenitor cell-mediated *de novo* regeneration of dental pulp with newly deposited continuous layer of dentin in an *in vivo* model. *Tissue Eng Part A* **16**, 605, 2010.
5. Huang, G.T., Gronthos, S., and Shi, S. Mesenchymal stem cells derived from dental tissues vs. those from other sources: their biology and role in regenerative medicine. *J Dent Res* **88**, 792, 2009.
6. Peng, L., Ye, L., and Zhou, X.D. Mesenchymal stem cells and tooth engineering. *Int J Oral Sci* **1**, 6, 2009.
7. Volponi, A.A., Pang, Y., and Sharpe, P.T. Stem cell-based biological tooth repair and regeneration. *Trends Cell Biol* **20**, 715, 2010.
8. Sonoyama, W., Liu, Y., Yamaza, T., Tuan, R.S., Wang, S., Shi, S., and Huang, G.T. Characterization of the apical papilla and its residing stem cells from human immature permanent teeth: a pilot study. *J Endod* **34**, 166, 2008.
9. Bakopoulou, A., Leyhausen, G., Volk, J., Tsiftoglou, A., Garefis, P., Koidis, P., and Geurtsen, W. Comparative analysis of *in vitro* osteo/odontogenic differentiation potential of human dental pulp stem cells (DPSCs) and stem cells from the apical papilla (SCAP). *Arch Oral Biol* **56**, 709, 2011.
10. Murray, P.E., Garcia-Godoy, F., and Hargreaves, K.M. Regenerative endodontics: a review of current status and a call for action. *J Endod* **33**, 90, 2007.
11. Agata, H., Sumita, Y., Asahina, I., Tojo, A., and Kagami, H. Ischemic culture of dental pulp-derived cells is a useful model in which to investigate mechanisms of post-ischemic tissue recovery. *Histol Histopathol* **28**, 985, 2013.
12. Aranha, A.M., Zhang, Z., Neiva, K.G., Costa, C.A., Hebling, J., and Nor, J.E. Hypoxia enhances the angiogenic potential of human dental pulp cells. *J Endod* **36**, 1633, 2010.
13. Zhou, H., Yang, Y.H., Binmadi, N.O., Proia, P., and Basile, J.R. The hypoxia-inducible factor-responsive proteins semaphorin 4D and vascular endothelial growth factor promote tumor growth and angiogenesis in oral squamous cell carcinoma. *Exp Cell Res* **318**, 1685, 2012.
14. Maes, C., Carmeliet, G., and Schipani, E. Hypoxia-driven pathways in bone development, regeneration and disease. *Nat Rev Rheumatol* **8**, 358, 2012.
15. Vihanto, M.M., Plock, J., Ermi, D., Frey, B.M., Frey, F.J., and Huynh-Do, U. Hypoxia upregulates expression of Eph receptors and ephrins in mouse skin. *FASEB J* **19**, 1689, 2005.
16. Salvucci, O., and Tosato, G. Essential roles of EphB receptors and EphrinB ligands in endothelial cell function and angiogenesis. *Adv Cancer Res* **114**, 21, 2012.
17. Luukko, K., Loes, S., Kvinnsland, I.H., and Kettunen, P. Expression of ephrin-A ligands and EphA receptors in the developing mouse tooth and its supporting tissues. *Cell Tissue Res* **319**, 143, 2005.
18. Dissanayaka, W.L., Zhan, X., Zhang, C., Hargreaves, K.M., Jin, L., and Tong, E.H. Coculture of dental pulp stem cells with endothelial cells enhances osteo-/odontogenic and angiogenic potential *in vitro*. *J Endod* **38**, 454, 2012.
19. Janebodin, K., Zeng, Y., Buranaphatthana, W., Ieronimakis, N., and Reyes, M. VEGFR2-dependent angiogenic capacity of pericyte-like dental pulp stem cells. *J Dent Res* **92**, 524, 2013.
20. Cheng, G., Liao, S., Kit-Wong, H., Lacorre, D.A., di-Tomaso, E., Au, P., Fukumura, D., Jain, R.K., and Munn, L.L. Engineered blood vessel networks connect to host vasculature via wrapping-and-tapping anastomosis. *Blood* **118**, 4740, 2011.
21. Lin, R.Z., and Melero-Martin, J.M. Fibroblast growth factor-2 facilitates rapid anastomosis formation between bioengineered human vascular networks and living vasculature. *Methods* **56**, 440, 2012.
22. Katsu, M., Koyama, H., Maekawa, H., Kurihara, H., Uchida, H., and Hamada, H. *Ex vivo* gene delivery of ephrin-B2 induces development of functional collateral vessels in a rabbit model of hind limb ischemia. *J Vasc Surg* **49**, 192, 2009.
23. Lu, F., Zhao, X., Wu, J., Cui, Y., Mao, Y., Chen, K., Yuan, Y., Gong, D., Xu, Z., and Huang, S. MSCs transfected with hepatocyte growth factor or vascular endothelial growth factor improve cardiac function in the infarcted porcine heart by increasing angiogenesis and reducing fibrosis. *Int J Cardiol* **6**, 2524, 2013.
24. Jabbarzadeh, E., Starnes, T., Khan, Y.M., Jiang, T., Wirtel, A.J., Deng, M., Lv, Q., Nair, L.S., Doty, S.B., and Laurencin, C.T. Induction of angiogenesis in tissue-engineered scaffolds designed for bone repair: a combined gene therapy-cell transplantation approach. *Proc Natl Acad Sci U S A* **105**, 11099, 2008.
25. Lutolf, M.P., and Hubbell, J.A. Synthetic biomaterials as instructive extracellular microenvironments for morphogenesis in tissue engineering. *Nat Biotechnol* **23**, 47, 2005.
26. Chen, X., Aledia, A.S., Popson, S.A., Him, L., Hughes, C.C., and George, S.C. Rapid anastomosis of endothelial progenitor cell-derived vessels with host vasculature is promoted by a high density of cotransplanted fibroblasts. *Tissue Eng Part A* **16**, 585, 2010.
27. Verseijden, F., Posthumus-van Sluijjs, S.J., van-Neck, J.W., Hofer, S.O., Hovius, S.E., and van-Osch, G.J. Vascularization of prevascularized and non-prevascularized fibrin-based human adipose tissue constructs after implantation in nude mice. *J Tissue Eng Regen Med* **6**, 169, 2012.
28. Laschke, M.W., Vollmar, B., and Menger, M.D. Inosculation: connecting the life-sustaining pipelines. *Tissue Eng Part B* **15**, 455, 2009.
29. Chen, X., Aledia, A.S., Ghajar, C.M., Griffith, C.K., Putnam, A.J., Hughes, C.C., and George, S.C. Prevascularization of a fibrin-based tissue construct accelerates the formation of functional anastomosis with host vasculature. *Tissue Eng Part A* **15**, 1363, 2009.
30. Wang, J., Liu, B., Gu, S., and Liang, J. Effects of Wnt/ $\beta$ -catenin signaling on proliferation and differentiation of apical papilla stem cells. *Cell Prolif* **45**, 121, 2012.
31. Saleh, F.A., Whyte, M., Ashton, P., and Genever, P.G. Regulation of mesenchymal stem cell activity by endothelial cells. *Stem Cells Dev* **20**, 391, 2011.
32. Bouletreau, P.J., Warren, S.M., Spector, J.A., Peled, Z.M., Gerrets, R.P., Greenwald, J.A., and Longaker, M.T. Hypoxia and VEGF upregulate BMP-2 Mrna and protein expression in microvascular endothelial cells: implications for fracture healing. *Plast Reconstr Surg* **109**, 2384, 2002.
33. Liu, L., Ling, J., Wei, X., Wu, L., and Xiao, Y. Stem cell regulatory gene expression in human adult dental pulp and periodontal ligament cells undergoing odontogenic/osteogenic differentiation. *J Endod* **35**, 1368, 2009.
34. Spath, L., Rotilio, V., Alessandrini, M., Gambarà, G., De Angelis, L., Mancini, M., Mitsiadis, T.A., Vivarelli, E., Naro, F., Filippini, A., and Papaccio, G. Explant-derived human dental pulp stem cells enhance differentiation and proliferation potentials. *J Cell Mol Med* **14**, 1635, 2010.

35. Grando Mattuella, L., Westphalen Bento, L., de Figueiredo, J.A., Nor, J.E., de Araujo, F.B., and Fossati, A.C. Vascular endothelial growth factor and its relationship with the dental pulp. *J Endod* **33**, 524, 2007.
36. Kertesz, N., Krasnoperov, V., Reddy, R., Leshanski, L., Kumar, S.R., Zozulya, S., and Gill, P.S. The soluble extracellular domain of EphB4 (sEphB4) antagonizes EphB4-ephrinB2 interaction, modulates angiogenesis, and inhibits tumor growth. *Blood* **107**, 2330, 2006.
37. Zhang, S., Jiang, T., and Liang, M. Expression of EphB4 and ephrinB2 in cervical cancer tissues and angiogenesis. *Int J Gynaecol Obstet* **96**, 46, 2007.
38. Gerety, S.S., and Anderson, D.J. Cardiovascular ephrinB2 function is essential for embryonic angiogenesis. *Development* **129**, 1397, 2002.
39. Reissenweber, B., Mosch, B., and Pietzsch, J. Experimental hypoxia does not influence gene expression and protein synthesis of Eph receptors and ephrin ligands in human melanoma cells *in vitro*. *Melanoma Res* **23**, 85, 2013.
40. Greenbaum, D., Colangelo C., Williams K., and Gerstein, M. Comparing protein abundance and mRNA expression levels on a genomic scale. *Genome Biol* **4**, 117, 2003.
41. Dery, M.A., Michaud, M.D., and Richard, D.E. Hypoxia-inducible factor 1: regulation by hypoxic and non-hypoxic activators. *Int J Biochem Cell Biol* **37**, 535, 2005.
42. Sohl, M., Lanner, F., and Farnebo, F. Sp1 mediate hypoxia induced ephrinB2 expression via a hypoxia-inducible factor independent mechanism. *Biochem Biophys Res Commun* **391**, 24, 2010.
43. Das, A., Shergill, U., Thakur, L., Sinha, S., Urrutia, R., Mukhopadhyay, D., and Shah, V.H. EphrinB2/EphB4 pathway in hepatic stellate cells stimulates Erk-dependent VEGF production and sinusoidal endothelial cell recruitment. *Am J Physiol Gastrointest Liver Physiol* **298**, 908, 2010.
44. Wang, F.S., Wang, C.J., Chen, Y.J., Chang, P.R., Huang, Y.T., Sun, Y.C., Huang, H.C., Yang, Y.J., and Yang, K.D. Ras induction of superoxide activates ERK-dependent angiogenic transcription factor HIF-1alpha and VEGF-A expression in shock wave-stimulated osteoblasts. *J Biol Chem* **279**, 10331, 2004.
45. Hainaud, P., Contreres, J.O., Villemain, A., Liu, L.X., Plouet, J., Tobelem, G., and Dupuy, E. The role of the vascular endothelial growth factor-Delta-like 4 ligand/Notch4-ephrin B2 cascade in tumor vessel remodeling and endothelial cell functions. *Cancer Res* **66**, 8501, 2006.
46. Yang, C., Guo, Y., Jadlovec, C.C., Li, X., Lv, W., Model, L.S., Collins, M.J., Kondo, Y., Muto, A., Shu, C., and Dardik A. Vascular endothelial growth factor-A inhibits EphB4 and stimulates delta-like ligand 4 expression in adult endothelial cells. *J Surg Res* **183**, 478, 2013.

Address correspondence to:  
Chengfei Zhang, DDS, PhD  
Comprehensive Dental Care, Endodontics  
Faculty of Dentistry  
The University of Hong Kong  
Hong Kong 999077  
China

E-mail: zhangcf@hku.hk

Received: January 21, 2014

Accepted: November 5, 2014

Online Publication Date: December 22, 2014